J. Phys. IV France **1** (2006) Pr1-1

Simulating Non-Equilibrium Dynamics of Molecules Confined in Zeolite Nanopores: Effects of Implicit and Explicit Thermostats on Microwave Heated Fluids

Aldo F. Combariza[1], Ethan Sullivan[1] and Scott M. Auerbach[2]

[1] *Department of Chemistry, University of Massachusetts Amherst, Amherst, MA 01003*

[2] *Department of Chemistry and Department of Chemical Engineering, University of Massachusetts Amherst, Amherst, MA 01003*

Abstract

We have simulated the non-equilibrium dynamics of methanol adsorbed in FAU zeolite driven by external microwave (MW) radiation. We have modelled steady states produced by augmenting this MW-driven system with a thermostat that acts as a balancing heat sink. We have compared results from an implicit thermostat (Andersen velocity replacement) and an explicit thermostat (helium atoms subjected to Andersen velocity replacement). We find very good agreement between the implicit and explicit thermostats for energy distributions and diffusion coefficients produced under MW-heated steady-state conditions. This augurs well for the continued use of implicit thermostats, which are computationally more efficient.

1 INTRODUCTION

The dynamics of molecules confined in nanopores plays a central role in reactions and separations that take place in zeolite cavities [1]. During the past few years, a flurry of interest has emerged in using microwave-heated zeolites in chemical processes, such as catalyst synthesis [2–6], ion exchange [7], reactions [8, 9] and separations [10, 11]. For example, Turner *et al.* [11] have recently studied the effects of microwave (MW) heating on a binary mixture of cyclohexane and methanol adsorbed in siliceous zeolites FAU and MFI [12]. They produced MW-heated steady states by running a bath gas of helium through the zeolite-guest sytems. Turner *et al.* found that the effect on sorption selectivity from conventional heating can be reversed by applying MW radiation. Despite such intriguing results, there remains disagreement whether MW-driven systems really behave in ways that are qualitatively different from conventionally heated systems [3,13,14]. This disagreement is fueled by the lack of a fundamental, atomistic picture for such MW-driven systems.

In recent work, we explored the nature of energy distributions in MW-driven zeolite systems using non-equilibrium molecular dynamics (MD) techniques [15–18]. We found that in MW-driven systems, it is possible to maintain benzene and methanol (see Fig. 1) at statistically different temperatures, suggesting that MW heating may produce novel athermal effects. Such effects arise in part from the dynamics of confinement in zeolite nanopores. Collisions between MW-excited guest molecules and zeolite cage walls serves to randomize the MW-excitation energy, leading to selective heating of certain degrees of freedom in the zeolite-guest system.

In our previous calculations, we simulate steady states by balancing energy inputs and outputs, with the inputs coming from the MW field. In our previous calculations, we simulated the removal of energy from the system by applying the Andersen thermostat, which replaces the three-dimensional velocities of randomly selected atoms at random times with those from appropriate Maxwell-Boltzmann distributions [19]. These replacements model the effect of collisions assuming instantaneous energy transfer with bath gas particles. While stochastic velocity-replacement likely reflects the microscopic dynamics of cooling in this system, the assumption of instantaneous energy transfer might influence the resulting energy distributions at steady state. To address this issue, we develop and apply in the present article an explicit helium thermostat for comparison with the more implicit Andersen thermostat. We find below that energy distributions and self-diffusion coefficients obtained from the helium thermostat are in broad agreement with those from the Andersen thermostat, suggesting that the assumption of instantaneous energy transfer does not contaminate our simulated MW-heated steady states.

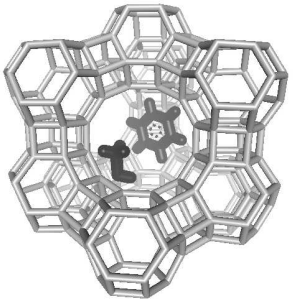

Figure 1. Schematic of FAU zeolite structure with adsorbed benzene and methanol.

The remainder of this article is organized as follows: in Sec. II we describe the interaction models and dynamics methods used to simulate MW-driven zeolites. In Sec. III we discuss the results of energy distributions and diffusion coefficients, and in Sec. IV we offer concluding remarks and suggestions for future work.

2 SIMULATION METHODS

In this section we describe the systems, interaction models and dynamics methods used to simulate MW-driven zeolites. We simulate the dynamics of methanol and helium confined in FAU zeolite (see Fig. 1), which features a cubic unit cell with a lattice parameter of 24.3 Å [20]. Each FAU unit cell contains 8 fully-formed cages, which are roughly spherical with a diameter of *ca.* 10 Å. Unless otherwise stated, the methanol loading was set to 16 molecules per unit cell (2 molecules per supercage). This loading level ensures enough statistics in the simulations discussed below. The helium loading was varied from 8 to 196 atoms to explore the influence of helium loading on thermostat performance.

2.1 Interactions

The potential energy has the form:

$$V = V_{\mathrm{Z}} + V_{\mathrm{M}} + V_{\mathrm{ZM}} + V_{\mathrm{MM}} + V_{\mathrm{ZH}} + V_{\mathrm{MH}} + V_{\mathrm{HH}} \tag{2.1}$$

where V_{Z}, V_{M}, V_{ZM} and V_{MM} are the potential energy functions representing zeolite flexibility, methanol flexibility, zeolite-methanol interactions, and methanol-methanol intermolecular interactions, respectively. Details about these potential functions and parameters can be found

in Ref. 16 and references therein. The additional terms V_{ZH}, V_{MH} and V_{HH} come into play when considering the helium thermostat. These terms treat zeolite-helium-, methanol-helium- and helium-helium interactions, respectively. All interactions involving helium are assumed to take the Lennard-Jones form:

$$V_{\mathrm{LJ}}(r) = 4\varepsilon \left[\left(\frac{\sigma}{r}\right)^{12} - \left(\frac{\sigma}{r}\right)^{6} \right]. \tag{2.2}$$

The values of σ and ε used in V_{ZH}, V_{MH} and V_{HH} are given in Table 1. The He-He values were taken from Ref. 21, while the He-zeolite values were calculated by Talu and Myers [22] using the standard combination rules: $\varepsilon_{ij} = \sqrt{\varepsilon_{ii}\varepsilon_{jj}}$ and $\sigma_{ij} = (\sigma_{ii}+\sigma_{jj})/2$. The He-methanol values were obtained using the same combination rules, using pure-component methanol parameters reported previously by us [16], as modified from the CVFF forcefield [23].

Species (i,j)	ε_{ij}(meV)	σ_{ij}(Å)
He-C	1.260	3.258
He-H[a]	1.244	2.545
He-H[b]	0	0
He-O[c]	3.062	2.747
He-Si	0	0
He-O[d]	2.413	2.952
He-He	0.939	2.640

Table 1. Lennard-Jones parameters for helium-methanol-, helium-zeolite- and helium-helium interactions. ([a]Methyl hydrogen in methanol; [b]Hydroxyl hydrogen in methanol; [c]Oxygen in methanol; [d]Oxygen in FAU zeolite.)

2.2 Dynamics

All molecular dynamics (MD) simulations were performed with our program DIZZY [24]. Periodic boundary conditions were enforced via the minimum image convention [25]. Short-range interactions were cut-off and shifted at 12 Å, and long-range electrostatic interactions were computed using the Ewald summation. We employed the velocity Verlet algorithm to integrate Newton's equations with a time step of 1 fs. Total simulation times were at least 0.3 ns for energy distributions, and at least 10 ns for diffusion simulations.

To simulate the dynamics of zeolite-guest systems driven by MWs, we make the classical dipole approximation for the interaction between matter and light. We assume that the MW field points along the z-axis, and is homogeneous in space because its wavelength is huge compared to typical MD length scales. We consider a monochromatic electric field of the form $\vec{E}_t = E \cdot \hat{z} \cdot \cos(\omega t)$, where E is the MW field strength and ω is the MW frequency. Consistent with our previous MW simulations [15–18], we approximate that the zeolite-guest dipole moment can be represented by fixed point charges on all atoms in the system.

Given these approximations, Hamilton's equations of motion become:

$$\frac{d\vec{r}_i}{dt} = \frac{\vec{p}_i}{m_i} \qquad \frac{d\vec{p}_i}{dt} = -\frac{\partial V}{\partial \vec{r}_i} + q_i \cdot \vec{E}_t, \tag{2.3}$$

where $\vec{r}_i$ and $\vec{p}_i$ are the three-dimensional position and momentum of particle i, respectively, m_i and q_i are its mass and charge, and $V = V(\vec{r}_1, \vec{r}_2, \ldots, \vec{r}_N)$ is the zeolite-guest potential

energy function described above. The additional electrostatic force in Eq. (2.3), namely $q_i \cdot \vec{E}_t$, attempts to push charged particles to the left or right along the z-axis, depending upon the sign of the charge and the phase of the electric field. Such forces can excite vibrations of zeolite atoms and can excite external vibrations and librations of guest molecules in zeolites. Unless otherwise stated, the field strength was set to 1.8 V/Å. In our simulations of MW-heated diffusion, the field strength was varied from 0.4 to 1.8 V/Å to obtain different steady-state temperatures. We set ω to the blue end of the MW spectrum: 9.4×10^{11} s^{-1}.

Steady-state conditions are produced by introducing a thermostat to simulate the cooling that occurs in the actual experiment when bath gas particles (such as He) collide with MW-heated zeolite-guest particles on the inflow side of the system. We simulate this cooling in two ways: the first way, hereafter denoted the "Andersen thermostat," does not include helium atoms in the simulation; the second way, hereafter denoted the "helium thermostat," does include explicit helium atoms in the simulation. Here we describe our implementation of the Andersen and helium thermostats. The Andersen thermostat replaces the three-dimensional velocities of randomly selected atoms at random times, with those from appropriate Maxwell-Boltzmann distributions [19]. We implemented Andersen's thermostat in DIZZY by specifying three parameters: $T_{\rm ts}$, the target temperature; τ, the average time between velocity replacements; n, the number of particles influenced at each replacement. In practice, the ratio of Andersen parameters, τ/n, is sufficient to distinguish one Andersen thermostat from another. As in our previous work, we set $T_{\rm ts} = 300$ K and $\tau/n = 10$ fs per particle.

The new helium thermostat is simply the Andersen thermostat applied only to helium atoms present in a zeolite-guest-helium system. This allows for energy removal from the zeolite-methanol system in a more natural way, through collisional energy transfer to the helium phase, which in turn loses energy to the thermostat. In what follows, we refer to the Andersen thermostat as the one without helium, even though both thermostats involve Andersen velocity replacement. We have found that the performance of the helium thermostat is very sensitive to the number of helium atoms present, but is much less sensitive to the target temperature and the velocity replacement rate. Unless otherwise stated, we set $T_{\rm ts} = 300$ K and $\tau/n = 5$ fs per helium atom.

We investigated MW-heated energy distributions for methanol in FAU by extracting effective temperatures for FAU zeolite, methanol and helium phases. Effective temperatures were extracted by properly normalizing the kinetic energies of zeolite, methanol and helium. Some care must be taken in making appropriate comparisons between energy distributions obtained with the Andersen and helium thermostats, precisely because of the presence of helium in the latter case. The simplest way to solve this problem is to compare Andersen/helium systems with the same amount of total kinetic energy in the zeolite+methanol portion. Agreement between the Andersen and helium thermostats is obtained if they give the same partitioning of kinetic energy to the zeolite and methanol phases.

To explore MW-heated diffusion, mean-square displacements (MSDs) were calculated for each molecule with a time average according to:

$$\langle|\vec{r}(t) - \vec{r}(0)|^2\rangle \approx \frac{1}{N_{\rm MD} - n} \sum_{i=1}^{N_{\rm MD}-n} |\vec{r}(i+n) - \vec{r}(i)|^2, \tag{2.4}$$

where $t = n\Delta t$, Δt is the MD time step, and $N_{\rm MD}$ is the number of MD steps. Diffusion coefficients were extracted from long-time linear slopes of MSDs (divided by 6), being careful to ensure that these simulations accessed diffusional length and time scales. In all cases, linear MSDs were obtained for lengths well beyond the cage-to-cage length of *ca.* 10 Å.

3 RESULTS AND DISCUSSION

In this section we discuss energy distributions and diffusion coefficients obtained from MW-driven steady states of methanol in FAU zeolite. Figure 2 shows the success of the helium thermostat at equilibrating the FAU-methanol system at various target temperatures, using 40 helium atoms and an average replacement time of $\tau/n = 5$ fs per helium atom. Figure 3 shows temperature profiles extracted from a MW-driven steady state obtained with the new helium thermostat using 40 helium atoms, $T_{\rm ts} = 300$ K and $\tau/n = 5$ fs. In these calculations the MW field strength was set to 1.8 V/Å. The steady state remains robust for long times (longer than the time scale shown) with effective temperatures obeying the inequalities: $T_{\rm meth} > T_{\rm zeo} > T_{\rm He}$. This makes sense because methanol acts as the direct MW absorber, helium acts as the heat sink, and the zeolite is in the middle.

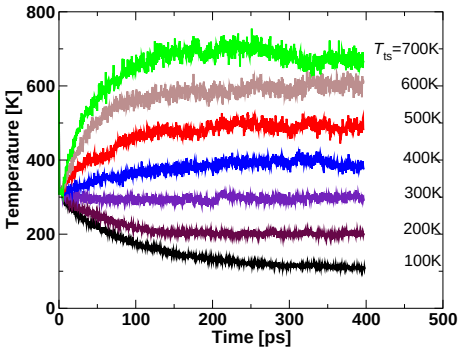

Figure 2. Thermal equilibrium states of zeolite-methanol-helium system produced with helium thermostat at various target temperatures $T_{\rm ts}$ (using 40 He, $\tau/n = 5$ fs).

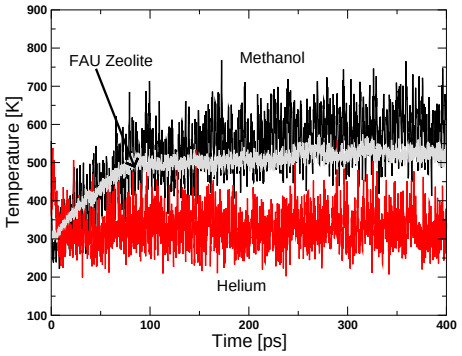

Figure 3. Time dependence of zeolite-, methanol- and helium-temperatures extracted from MW-driven steady state produced with the explicit helium thermostat (using 40 He, $T_{\rm ts} = 300$ K, $\tau/n = 5$ fs).

Figure 4 shows average temperatures of methanol, zeolite and helium obtained from helium thermostatted steady states, as a function of the number of heliums in the system. Figure 4 shows the remarkable fact that steady states can be obtained with as few as 10 helium atoms amidst 672 zeolite/methanol atoms. The strength of the thermostat increases with the number of heliums, with all three phases approaching the target temperature of 300 K with increasing

helium concentration. In what follows we focus on helium thermostats using between 24-40 helium atoms per FAU u

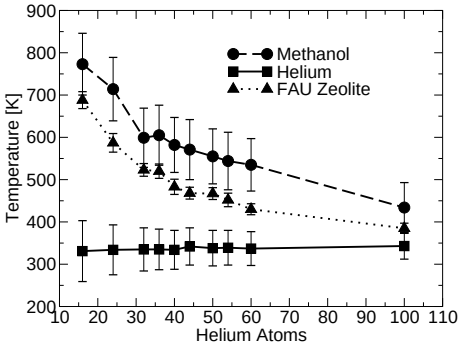

Figure 4. Dependence of MW-heated steady state temperatures on number of He atoms (using $T_{\rm ts} = 300$ K, $\tau/n = 5$ fs).

Figures 2–4 establish the usefulness of the helium thermostat for generating equilibrium states and MW-driven steady states. We presume that this thermostat treats energy transfer and cooling more faithfully than does the Andersen thermostat. Now we compare the predictions regarding energy distributions and diffusion from these two thermostats. Figure 5 shows kinetic energy distributions from MW-driven zeolite-methanol systems at steady state using the two thermostats. As discussed above, comparisons between the two thermostats only make sense when the amount of kinetic energy in the zeolite+methanol portion (denoted FAU+MeOH in Fig. 5) is the same. We see in Fig. 5 that when using the same target temperature ($T_{\rm ts} = 300$ K) and replacement time ($\tau/n = 10$ fs per particle), the Andersen and helium thermostats give steady states whose comparison is inappropriate, because the kinetic energies in the zeolite+methanol portion are quite different. In contrast, using Andersen parameters ($T_{\rm ts} = 340$ K, $\tau/n = 45$ fs per particle) and helium parameters (24 He, $T_{\rm ts} = 300$ K, $\tau/n = 5$ fs per helium) gives steady states with the same zeolite+methanol kinetic energy, as shown in Fig. 5. Also shown in Fig. 5 is the fact that both thermostats give the same distribution of energy between the zeolite and methanol, with the methanol phase roughly 100 K hotter than the zeolite. This agreement lends confidence to our treatment of cooling in MW-driven non-equilibrium states.

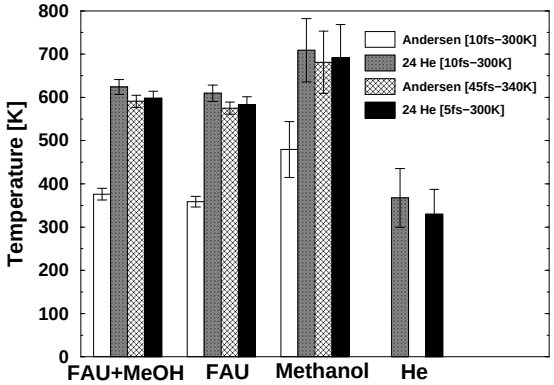

Figure 5. Comparison of energy distributions obtained using implicit (Andersen) and explicit (He) thermostats.

As a further test of the agreement between these two thermostats, we show in Fig. 6 methanol self-diffusion coefficients computed at equilibrium and under steady-state conditions using the two thermostats. The equilibrium and MW-driven/Andersen self-diffusivities were reported previously by us [17]. The MW-driven/Andersen diffusivities were computed with MW field strengths of (0.5, 1.0, 1.5 V/Å), and with Andersen parameters ($T_{\rm ts}$ = 300 K, τ/n = 10 fs). The MW-driven/helium diffusivities were computed with MW field strengths of (0.4, 0.8, 1.2, 1.8 V/Å), and with helium parameters (24 He, $T_{\rm ts}$ = 300 K, τ/n = 5 fs). For the MW-driven systems, the temperatures were extracted from the total kinetic energy of methanol (translation, rotation and vibration).

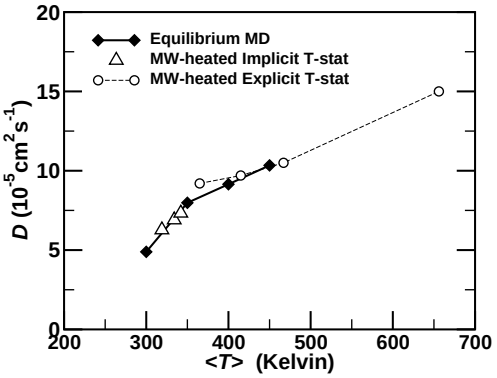

Figure 6. Comparison of self-diffusion coefficients of methanol in FAU zeolite (8 molecules per cell), from: equilibrium molecular dynamics, MW-heated steady-state dynamics with an implicit (Andersen) thermostat, and MW-heated steady-state dynamics with an explicit (helium) thermostat. (using 24 He, $T_{\rm ts}$ = 300 K, τ/n = 5 fs).

In our previously reported work on MW-driven diffusion [17], we suggested a picture of different guests diffusing at different MW-driven temperatures. As such, for a system thermostatted at 300 K and with a steady-state MW-driven temperature of 350 K, the self-diffusivity found from MD agrees with the equilibrium value at 350 K. This concept is manifested in Fig. 6 by the overlay of the upright triangles (MW/Andersen) and the solid line (equilibrium). As a test of agreement between MW/Andersen and MW/helium, we look for agreement between MW/helium self-diffusivities and those at corresponding equilibrium conditions. This is indeed found in Fig. 6 over the temperature range 350–450 K where equilibrium self-diffusion data were available prior to submission. Thus, we find excellent agreement between the two thermostats in both their energy distributions and their diffusional dynamics.

4 CONCLUDING REMARKS

We have simulated the non-equilibrium dynamics of methanol confined in FAU zeolite nanopores, driven by external microwave (MW) radiation. These simulations test whether athermal energy distributions are predicted for systems subjected to MW radiation. We have modelled steady states produced by augmenting this MW-driven system with a thermostat that acts as a balancing heat sink. We have compared results from an implicit thermostat (Andersen velocity replacement) and an explicit thermostat (helium atoms subjected to Andersen velocity

replacement). We find very good agreement between the implicit and explicit thermostats for energy distributions and diffusion coefficients produced under MW-heated steady-state conditions. This agreement lends confidence to our treatment of cooling in these non-equilibrium systems.

In future work we plan to simulate the distribution of MW-excitation into translational, rotational and vibrational modes, for comparison with corresponding neutron scattering experiments.

5 ACKNOWLEDGMENTS

We thank Prof. W. Curtis Conner, Jr. for enlightening discussions regarding microwaves. We also thank Dr. H. Jobic and the Institut de Recherches sur la Catalyse, Villeurbanne, France, for generously supporting S.M.A.'s attendance at the 3rd International Workshop on Dynamics in Confinement – Confit2006, held in Grenoble, France at the Institut Laue-Langevin. We are also grateful for generous funding from the National Science Foundation Nanoscale Interdisciplinary Research Team program (grant number CTS-0304217).

References

[1] S. M. Auerbach, K. A. Carrado, and P. K. Dutta, editors, *Handbook of Zeolite Science and Technology*, Marcel Dekker, Inc., New York, 2003.
[2] S. Mintova, S. Mo, and T. Bein, Chem. Mater. **10**, 4030 (1998).
[3] C. S. Cundy, Collect. Czech. Chem. Commun. **63**, 1699 (1998).
[4] K. J. Rao, B. Vaidhyanathan, M. Ganguli, and P. A. Ramakrishnan, Chem. Mater. **11**, 882 (1999).
[5] W. C. Conner, G. Tompsett, K. H. Lee, and K. S. Yngvesson, J. Phys. Chem. B **108**, 13913 (2004).
[6] G. A. Tompsett, W. C. Conner, and S. Yngvesson, Chem. Phys. Chem. **7**, 296 (2006).
[7] J. M. Lopes, F. N. Serralha, C. Costa, F. Lemos, and R. Ribeiro, Catal. Lett. **53**, 103 (1998).
[8] M. Hajek, Collect. Czech. Chem. Commun. **62**, 347 (1996).
[9] C. Marun, L. D. Conde, and S. L. Suib, J. Phys. Chem. A **103**, 4332 (1999).
[10] S. Kobayashi, Y.-K. Kim, C. Kenmizaki, S. Kushiyama, and K. Mizuno, Chem. Lett. **9**, 769 (1996).
[11] M. D. Turner, R. L. Laurence, W. C. Conner, and K. S. Yngvesson, AIChE J. **46**, 758 (2000).
[12] C. Baerlocher, W. M. Meier, and D. H. Olson, *Atlas of Zeolite Framework Types*, Elsevier, Amsterdam, fifth edition, 2001, <http://www.iza-structure.org/databases>.
[13] D. A. C. Stuerga and P. Gaillard, J. Microwave Power Electromagn. Energy **31**, 87 (1996).
[14] D. A. C. Stuerga and P. Gaillard, J. Microwave Power Electromagn. Energy **31**, 101 (1996).
[15] C. Blanco and S. M. Auerbach, J. Am. Chem. Soc. **124**, 6250 (2002).
[16] C. Blanco and S. M. Auerbach, J. Phys. Chem. B **107**, 2490 (2003).
[17] C. Blanco and S. M. Auerbach, J. Comput. Theor. Nanosci. **1**, 180 (2004).
[18] A. F. Combariza, E. Sullivan, S. M. Auerbach, and C. Blanco, J. Phys. Chem. B **109**, 18439 (2005).
[19] H. C. Andersen, J. Chem. Phys. **72**, 2384 (1980).
[20] J. A. Hriljac, M. M. Eddy, A. K. Cheetham, J. A. Donohue, and G. J. Ray, J. Solid State Chem. **106**, 66 (1993).
[21] J. O. Hirschfelder, C. F. Curtiss, and R. B. Bird, *Molecular Theory of Gases and Liquids*, Wiley, New York, 1954.
[22] O. Talu and A. L. Myers, Coll. and Surf. A **187-188**, 83 (2001).
[23] Biosym/MSI, San Diego, *Discover 2.9.7 / 95.0 / 3.0.0 User Guide*, 1995.
[24] N. J. Henson, PhD thesis, Oxford University, 1996.
[25] M. F. Allen and D. J. Tildesley, *Computer Simulation of Liquids*, Oxford Science Publications, Oxford, 1987.